Cytometry 29:41–49 (1997)

Early Endosome Membrane Dynamics Characterized by Flow Cytometry

Philippe Chavrier,[1] Peter van der Sluijs,[2] Zohair Mishal,[3] Bas Nagelkerken,[2] and Jean-Pierre Gorvel[1]*

[1]Centre d'Immunologie INSERM-CNRS de Marseille-Luminy, Marseille, France
[2]Department of Cell Biology, Utrecht University School of Medicine, Utrecht, The Netherlands
[3]Centre de Soutien pour la Recherche sur le Cancer, Villejuif, France

Received 16 November 1996; Accepted 26 February 1997

Early endosomes are very dynamic intracellular membrane organelles that undergo multiple fusion and fission events. In this study, we developed a novel assay based on multiparametric flow cytometric analyses and early endosome sorting to characterize better the mechanisms of early endosome membrane dynamics in vitro. In particular, we have investigated the role of rab4 and rab5, two small GTPases known to regulate distinct steps of membrane traffic in the endocytic pathway. We show that early endosomes undergo homotypic fusion reactions, which lead to the formation of fusion intermediates with increased size. Fusion is efficiently stimulated by recombinant rab5 but not by recombinant rab4. Subsequently, membrane fission consumes this larger fusion compartment. This fission process is stimulated by rab4 and by the GTP hydrolysis-defective mutant rab4Q67L. Cytometry 29:41–49, 1997. © 1997 Wiley-Liss, Inc.

Key terms: endocytosis; membrane fusion; membrane fission; rab4; rab5

In vitro reconstitution systems have provided important insights into the mechanisms of intracellular membrane transport (9,24). Particularly, the reconstitution of vectorial transport between the endoplasmic reticulum and the Golgi apparatus and within the Golgi apparatus has provided an impressive advance in our understanding of the molecular mechanisms of vesicular transport. The identification of families of proteins that are conserved between yeast and humans has defined the outline of what appears to be a unifying concept for vesicular transport, which may serve as a paradigm for membrane transport between distinct intracellular compartments (12,24,25). Although the individual steps making up the endocytic route are fairly well understood at the descriptive level, the reconstitution of the endocytic pathway has not yet evolved to a similar degree of completion as for the biosynthetic route. It is clear that early endosomes exhibit a high propensity to undergo homotypic fusion (12). This process is specific, because early endosomes do not fuse with late endocytic structures (1). Early endosome fusion involves the N-ethylmaleimide-sensitive factor (23), trimeric G proteins, and small GTPases of the rab and arf families (7,11,17,20).

The efficient in vitro fusion activity of early endosomes indicates that this compartment is highly dynamic in vivo (13). Morphological observations at ultrastructural and light microscopic levels suggested that early endosomes are organized as a tubulovesicular network (30). The plasticity and dynamics (16) of this tubulovesicular system are thought to depend on the capacity of individual early endosomes to undergo fusion and fission events in vivo to maintain a steady-state composition of membrane and resident proteins (12).

We previously localized rab4 and rab5, two members of the rab family of small GTPases, together with the transferrin receptor in the early endosomal network (4,33). It is not surprising that the early endosomal compartment contains several rab GTPases (19), each of which possibly controls a distinct transport event leading to or originating from the early endosome. Early endosomes receive contents of incoming coated vesicles, recycle material to the plasma membrane via the recycling compartment, and route other materials to late endosomes (22). A possible role for rab5 was initially inferred from in vitro endosome fusion experiments in which this GTPase was shown to enhance lateral homotypic early endosome fusion (11). Two point mutations in rab5 that impair binding of GTP, rab5S22N and rab5N133I, inhibit early endosome fusion (11,28). In vivo functional analysis of endocytosis in rab5 transfectants confirmed and extended the results from the in vitro fusion assays. Overexpression of rab5 or activating

Contract grant sponsor: CNRS; Contract grant sponsor: INSERM; Contract grant sponsor: Association de la Recherche contre le Cancer; Contract grant sponsor: Stichting ''De Drie Lichten''; Contract grant sponsor: The Netherlands Organization of Medical Research.

*Correspondence to: Dr. Jean-Pierre Gorvel, Centre d'Immunologie de Marseille-Luminy, Case 906, 13288 Marseille, France.
E-mail: gorvel@ciml.univ-mrs.fr

mutations such as the GTPase-deficient rab5Q79L increases the size of the early endosomes and the rate of endocytosis (3). In contrast, the dominant negative rab5S22N and rab5N133I mutants both inhibit endocytosis (3,28) and cause fragmentation of early endosomes as evidenced by light and electron microscopy (3).

The role of rab4 in endocytosis has not been investigated in the same detail as rab5, because a particular step that is rab4 dependent has not been reconstituted as yet. We previously started to address the role of rab4 in vivo by generating stable cell lines expressing wild-type or mutant rab4. Through morphological studies and a detailed kinetic analysis of the uptake, sorting, recycling, and degradation of several endocytic tracers in Chinese hamster ovary cells transfected with wild-type or mutant rab4, we concluded that rab4 plays a critical, but incompletely understood, role in the recycling of transferrin receptor and fluid-phase markers through the early endosomal compartments (6,35). Our recent functional morphological analysis using immunogold electron microscopy and confocal immunofluorescence suggests that rab4 is specifically involved in transport between sorting and recycling endosomes and not between the recycling endosomes and plasma membrane (6).

In this study, we used an in vitro reconstitution assay to investigate early endosome membrane dynamics. We found that early endosomes undergo homotypic fusion reactions that lead to the formation of fusion intermediates with increased size. Fusion is efficiently stimulated by recombinant rab5 but not by recombinant rab4. Subsequently, membrane fission consumes this larger fusion compartment. Interestingly, we observed that the endosomal fission process is stimulated by rab4 and by the GTP hydrolysis-defective mutant rab4Q67L but not by a rab4S22N mutant with impaired GTP binding. These data suggest that early endosomes are highly dynamic organelles whose composition is governed by membrane fusion and fission events, the control of which is ensured by at least two GTPases of the rab family.

MATERIALS AND METHODS

Cells and Antibodies

Baby hamster kidney (BHK-21) cells were maintained and seeded for experiments as previously described (13). The affinity-purified rabbit antibodies against rab5 or rab4 were previously characterized (4,34). The murine monoclonal anti-rab5 antibody was a gift from J. Gruenberg, University of Geneva; the rabbit polyclonal anti-human CD26 antibody from S. Maroux, University of St. Jérome, Marseilles; the murine antilysozyme antibody from L. Leserman, CIML, Marseilles; and the mouse monoclonal anti-GST ND2.1 from N. Gruel, Institut Curie, Paris.

Preparation of Fluorescent Early-Endosome-Enriched Fractions

Bovine serum albumin (BSA; Sigma, St. Louis, MO) was labeled with fluorescein-5′-isothiocyanate (FITC) or tetramethylrhodamine isothiocyanate (TRITC; Molecular Probes, Eugene, OR) to a stoichiometry of 1 mol dye per mol protein (10). For fluorescence resonance energy transfer (FRET) experiments, labeling of BSA to fluorescein and rhodamine was carried out as described elsewhere (10). Molar dye-to-protein ratios of 1–3 were obtained for fluorescein and between 1 and 4 for rhodamine using spectrophotometry. FITC-BSA or TRITC-BSA was dialyzed against MEM culture medium containing 10 mM Hepes, 5 mM D-glucose, pH 7.4, prior to experiments. TRITC-BSA or FITC-BSA (20 mg/ml) was incubated for 5 min at 37°C in BHK-21 cells, the time required to label the compartments of the early endocytic pathway. After five 10 min washes at 4°C with BSA 0.5% in phosphate-buffered saline, pH 7.4 (PBS), and one wash with PBS only, cells were scraped from eight 10-cm-diameter confluent plates and homogenized in 250 mM sucrose, 3 mM imidazole, pH 7.4. After homogenization and preparation of a postnuclear supernatant (PNS; 11,13), a sucrose step flotation gradient was used to prepare early-endosome-enriched membranes (EE; 11). Briefly, the PNS was brought to 40.6% sucrose and 0.5 mM EDTA, loaded at the bottom of a SW60 tube, and sequentially overlaid with 1.5 ml 35% sucrose in 3 mM imidazole, pH 7.4, containing 0.5 mM EDTA; 1 ml 25% sucrose in 3 mM imidazole, pH 7.4, containing 0.5 mM EDTA; and 0.5 ml of homogenization buffer. The gradient was run for 60 min at 124,000*g* in a SW60 swinging rotor (r_{av} 91.7 mm). The early-endosome-enriched membrane fraction (EE) was collected at the 25–35% sucrose interface. Concentrated cytosol (12 mg/ml of protein) was prepared from BHK-21 cells as previously described (11). Protein concentrations were also determined as previously described (2).

Cell-Free Assay

For each in vitro assay, 50 µl aliquots (25 µg protein) of the FITC-BSA and of the TRITC-BSA containing EE were gently mixed with 50 µl of cytosol, adjusted to 12.5 mM HEPES (pH 7.4), 1.5 mM $Mg(OAc)_2$, 3 mM imidazole, 1 mM DTT, 50 mM KOAc, complemented with an ATP-regenerating system (1:1:1 mixture of 100 mM ATP, pH 7.0, 800 mM creatine phosphate, and 4 mg/ml creatine phosphokinase) and 8 µM geranylgeranyl-pyrophosphate (ARC, St Louis, MO). Assays were supplemented with 1.5 µg of recombinant rab proteins. Cell-free assays were initiated by gently mixing the samples on ice. After 10 min at 4°C, samples were transferred to 37°C. At the indicated time points, samples were chilled to 4°C and the volume was adjusted to 500 µl with ice-cold PBS.

Three-Color Analysis System

After in vitro assays, the reaction mixtures were cooled to 4°C. The incubation was continued for 30 min at 4°C in the presence of 5 µg/ml affinity-purified rab4 or rab5 antibodies and 1 µg/ml biotin-conjugated goat anti-rabbit Fab'_2 (Caltag, San Francisco, CA). Subsequently, 40 µg/ml final concentration of allophycocyanin (APC) conjugated to streptavidin (Caltag) was added for 30 min at 4°C. Samples were diluted to 3 ml with ice-cold PBS and analyzed in a Coulter Elite flow cytometer (Coulter Corp., Hialeah, FL). Statistical analyses of fluorochrome combina-

tions were done with the three-color PRISM parameter analysis software package of the Elite flow cytometer. For a three-color immunofluorescence analysis, eight possible combinations can be assigned to the different channels of a flow cytometer. We were interested in analyzing the percentage of endosomes containing the three markers (FITC-BSA, TRITC-BSA, and rab5 or rab4 as detected by the APC system). In channel 960, the elements containing all three dyes were detected. Statistical analyses were performed by considering either the total endosome population (1–7 μm relative diameter) or the population of small endosomes (1–3 μm relative diameter) or the population of large endosomes (3–7 μm relative diameter) obtained after 37°C in vitro assays. The flow cytometer was calibrated in the forward and right angle light scatter modes (FALS and 90LS, respectively) using fluorescent beads of 0.95 μm, 2 μm, and 5 μm. Under these conditions, the relative size of rab4- or rab5-positive elements used as an input in the assay and analyzed at 4°C in the absence of cytosol was 0.5–3 μm. A gate was chosen to select the rab5- or rab4-positive endosomes according to the APC channel. By gate addition, APC-positive structures contained 74% ± 15% of rab5-or rab4-positive early endosomes (without any gate, APC-positive early endosomal structures represented 30% ± 2% of the total number of elements). The filters setting for fluorescein was 525 nm Oriel (Oriel Corp., Stratford, CO) bandpass filter, for rhodamine a 580 nm Oriel bandpass filter, and for APC a 675 M.T.O. (Matériel et Travaux Optiques, Massy, France) bandpass filter. The laser excitations were 488 nm for fluorescein, 514 nm for rhodamine, and 633 nm for APC.

Plasmid Construction

Rab5 was extended with EcoRI sites in a polymerase chain reaction (PCR) using pGEMIrab5 (5) as template and the following primer set: 5′-gag-ggt-acc-gaa-ttc-atg-gct-aat-cga-gga-gca-aca-aga-ccc-aac-ggg-3′ (sense) and 5′-tc-tag-gga-tcc-gaa-ttc-tta-gtt-act-aca-ctg-act-cct-ggt-tgg-ctg-3′ (antisense). This PCR fragment was ligated into the EcoRI site of pGEX2T. Wild-type rab4 and the truncation mutant rab4CT3 lacking the carboxyterminal CGC prenylation motif were excised with EcoRI from BluescriptKS$^+$ and ligated into pGEX2T. The construction and biochemical characterization of epitope-tagged hydrolysis-deficient mutant rab4Q67L and of the GTP binding mutant rab4S22N will be described elsewhere. The rab4Q67L and rab4S22N cDNAs were cloned in the EcoRI of pGEX1λT and pGEX2T. All mutations and DNA sequences that were generated in PCRs were verified by dideoxy sequencing (26).

Purification of Glutathione S-Transferase Fusion Proteins and Biochemical Detection of rab Recombinant Proteins to EE Membrane

pGEX constructs were transformed into *Escherichia coli* DH5α. Bacteria were induced with 0.1 mM IPTG for 3 h at 37°C and subsequently lysed upon sonication in 1% Triton X-100/PBS containing 2.5 mM phenylmethylsulfonyl fluoride (PMSF). Recombinant fusion proteins were purified by affinity chromatography on glutathione agarose and eluted with 5 mM reduced glutathione. Eluates were washed and concentrated in Amicon miniconcentrators, assayed for protein content, and stored in small aliquots at −80°C. For GST-fusion protein detection in EE, 1.5 μg of GST or GSTrab4Q67L, GSTrab4S22N, GSTrab4CT3, or GSTrab5wt was added in the cell-free assay (see above) containing 100 μl of EE and 50 μl of cytosol for 10 min at 4°C, followed by 10 min at 37°C. Samples were then adjusted to 2 ml with 1 M NaCl in cold PBS, loaded on top of a 20% sucrose cushion in 1 M NaCl PBS, pH 7.4, and subjected to a 208,000*g* centrifugation for 30 min at 4°C in a TLA-100 centrifuge (Beckman, Palo Alto, CA). Membrane pellets and supernatants were then treated for SDS-PAGE. Proteins were loaded on 12% SDS-PAGE gels and transferred onto Immobilon-P membranes. Incubation steps with the mouse monoclonal anti-GST antibody were done in PBS with 5% dry milk and 0.05% Tween-20. Detection of GST and recombinant proteins recognized by the anti-GST antibody was performed using peroxidase-conjugated goat antimouse IgG antibodies (Immunotech, Marseilles, France) with the enhanced chemiluminescence system (ECL; Amersham, Les Ullis, France).

Sorting of Large EE

FITC-BSA or TRITC-BSA was internalized for 5 min at 37°C in BHK-21 cells and EE prepared from PNS by flotation gradient centrifugation. For each in vitro assay, a 100 μl aliquot (50 μg protein) of the FITC-BSA and a 100 μl aliquot (50 μg protein) of the TRITC-BSA containing EE were mixed with 100 μl of cytosol in the presence of an ATP-regenerating system and 8 μM geranylgeranyl-pyrophosphate. Cell-free assays were incubated for 10 min at 4°C, followed by 15 min at 37°C. Then, samples were chilled to 4°C and the volume was adjusted to 500 μl with ice-cold PBS. Before sorting, conditions were set up by analyzing a 50 μl aliquot from the 500 μl assay solution. Large EE were selected by gating on both the presence of FITC-BSA and TRITC-BSA contents as well as their 3–7 μm size in the light scatter mode. Although sorting was performed at room temperature, large EE were collected in 1 ml of ice-cold cytosol. A 300 μl aliquot was mixed with 1.5 μg GSTrab4Q67L and another 300 μl with 1.5 μg GSTrab4S22N; the third sample (300 μl control sample) did not contain any recombinant rab fusion protein. The samples were then subjected to a subsequent in vitro assay for 10 min at 37°C. At the end of the assays, 50 μl of each sample was diluted with 500 μl of cold PBS and analyzed by flow cytometry as described above.

Immunodetection of Both rab4 and rab5 on EE Membranes

EE were prepared as described above but from BHK-21 cells that were not previously incubated with the rhodamine and fluorescein BSA tracers. A 100 μl EE aliquot (50 μg protein) was incubated for 30 min at 4°C in the presence of 5 μg/ml affinity-purified antirab4 or murine monoclonal antirab5 antibodies, followed by a 30 min incubation at 4°C with a 1/1,000 dilution of both 1 mg/ml Fab′$_2$ goat anti-rabbit IgG fluorescein-labeled and Fab′$_2$

goat anti-mouse IgG rhodamine-labeled antibodies (Immunotech, Marseilles, France). At the end of incubations, 50 μl of the mixture was diluted 200 times with ice-cold PBS and analyzed with the Elite flow cytometer. In control samples, rabbit polyclonal antihuman CD26 and mouse monoclonal anti-lysozyme antibodies were used instead of rabbit antirab4 and mouse antirab5 antibodies, respectively. The laser excitations were at 488 nm for fluorescein and 514 nm for rhodamine. The flow cytometer was equipped with a conventional filter system for detecting the two fluorescent tracers.

FRET Experiments

Flow cytometric FRET measurements have been applied in a simplified form using a flow cytometer equipped with a single excitation beam (29). The FACS 440 flow cytometer (Becton Dickinson, San Jose, CA) was used to determine energy transfer between FITC-BSA and TRITC-BSA present in EE populations. According to Förster theory (8), an excited-state donor fluorophore can transfer energy over a long distance (nm) to an acceptor by nonradiative energy transfer, provided that 1) the quantum efficiency of the donor molecule is sufficiently high, 2) the excitation spectrum of the receptor overlaps with the emission spectrum of the donor, 3) the orientations of the transition moments of the donor and the acceptor are closely aligned, and 4) the distance between donor and acceptor is in the correct range (2–10 nm).

Equation 1 describes the functional dependence of the fluorescence resonance energy transfer efficiency, E, on the distance, R, between donor and acceptor:

$$E = R_0^{-6}/(R_0^{-6} + R^{-6}). \quad (1)$$

R_0 is a characteristic distance for a given donor-acceptor pair (fluorescein/rhodamine), with transfer efficiency of 50%. From the quenching of donor fluorescence, E can be determined as

$$E = 1 - Q_D^A/Q_D = 1 - I_D^A/I_D, \quad (2)$$

where $Q_D{}^A$ and Q_D are fluorescence quantum yields of the donor in the presence and absence of acceptor and $I_D{}^A$ and I_D are the fluorescence intensities of the donor in the presence and the absence of acceptor, respectively. The sensitization of the acceptor is given by

$$I_D^A/I_D = 1 - \epsilon_D C_D/\epsilon_A C_A E, \quad (3)$$

where $I_D{}^A$ and I_D are the fluorescence intensities of the acceptor in the presence and absence of donor, C_D and C_A are the molar concentrations, and ϵ_D and ϵ_A the molar absorption coefficients of the donor and acceptor, respectively, at the excitation wavelength. Equations 2 and 3 were applied to flow cytometric measurements, and population-averaged values for fluorescence intensities were used to give mean fluorescence values. With this method, the energy transfer efficiency E is evaluated for each endosome, from which a frequency distribution for the population can be generated. The flow cytometric measurements of E are carried out as follows. After in vitro assays, FITC-BSA served as a donor and TRITC-BSA served as acceptor. Fluorescence emitted from EE was detected with two photomultiplier tubes using a dichroic beam splitter and appropriate optical filters. Photomultiplier 1 detected the emitted light through use of a 535 nm bandpass filter and a OG 530 nm cutoff filter (I_1). Photomultiplier 2 detected fluorescence beyond 590 nm using a 580 nm dichroic filter and 590 cutoff filter (I_2). The excitation wavelength could be either 488 nm or 514 nm; both rhodamine and fluorescein are excited by these wavelengths. For simplicity, we introduce the notation $I(\lambda_1; \lambda_2)$, which is defined as fluorescence intensity measured at λ_2 nm, with excitation at λ_1 nm. Then, the measured intensities are described analytically by equations 4 and 5:

$$I_1(488 \text{ or } 514;540) = I_F(1 - E) + I_R S_4 \quad (4)$$

$$I_2(488 \text{ or } 514;580) = I_F(1 - E)\, S_1 + I_R + I_F E\alpha. \quad (5)$$

I_F and I_R are the theoretical directly excited fluorescence intensities of the fluorescein and rhodamine when no energy transfer occurs, and S_1 and S_4 are corrections for spectral overlap associated with direct excitation of the respective fluorophores. S_1, which is defined as I_2/I_1, is determined using endosomes that have endocytosed FITC-BSA, and S_4, which is defined as I_1/I_2, is determined with endosomes that have endocytosed TRITC-BSA, and α is determined as described elsewhere (31). Experimental values for $S_1 = 0.35$ with 488 nm excitation and $S_1 = 0.15$ with 514 nm excitation, $S_4 = 0.017$ with 488 nm excitation and $S_4 = 0.068$ with 514 nm excitation. As described elsewhere (29), E can be expressed as in equation 6:

$$E = \frac{I_2/I_1\,(1 + S_4 C_{R\in R}/C_{F\in F}\alpha) - S_1 - C_{R\in R}/C_{F\in F}\alpha}{I_2/I_1 - S_1 - \alpha}. \quad (6)$$

This term is suitable for determination of energy transfer efficiency values on an endosome-by-endosome basis, because all parameters on the right side can be measured separately or determined experimentally. C_R and C_F are the molar concentrations of TRITC and FITC and ϵR and ϵF their respective molar extinction coefficients. The C_R/C_F values were calculated from the initial composition of the incubation mixture of FITC-BSA and TRITC-BSA as described in detail elsewhere (15).

Thus, the proximity of labeled BSA is expressed as a frequency distribution histogram of E over the endosome population. BHK cells were incubated for 5 min at 37°C with 20 mg/ml of fluorescent markers. After cell homogenization, endosomes were prepared and used for in vitro assays (see above). Samples were incubated for 10 min at 4°C or for 15 min or 60 min at 37°C.

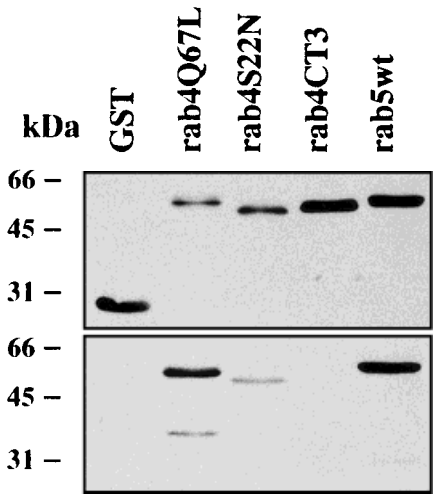

FIG. 1. GSTrab4Q67L, rab4S22N, and rab5wt recombinant proteins attach to EE membranes. One hundred microliters of EE were mixed with 50 µl of cytosol. Then, 1.5 µg of GST or recombinant proteins GST-rab4Q67L, -rab4S22N, -rab4CT3, or -rab5wt were added in the presence of 8 µM geranylgeranyl-pyrophosphate and each assay was incubated for 10 min at 4°C, followed by 10 min at 37°C. After centrifugation, high-speed membrane pellets (**lower panel**) and supernatants (**upper panel**) were then treated for SDS-PAGE. Proteins representing 1/400 of total supernatants and one-half of total membrane pellets were loaded on a 12% SDS-PAGE gel and transferred onto Immobilon-P membranes. GST and recombinant proteins were labeled with the anti-GST antibody and detected using peroxidase-conjugated goat anti-mouse IgG antibodies and enhanced chemiluminescence.

RESULTS

Recombinant rab Fusion Proteins Are Incorporated Into EE Membranes In Vitro

rab GTPases were expressed in *E. coli* as fusion proteins with an aminoterminal GST tag to allow their purification on a glutathione-agarose column. Purified GSTrab fusion proteins were added to the fusion assay in the presence of geranylgeranyl-pyrophosphate under conditions that allow prenylation of the carboxytermini of the bacterially produced proteins (18). We first addressed whether added recombinant rab proteins have the ability to associate with EE membranes during the 37°C incubations. Figure 1 shows that GSTrab4S22N with impaired GTP binding and the GTPase-defective mutant GSTrab4Q67L and GSTrab5wt fusion proteins all with intact prenylation motifs were associated with membrane pellets even after high-salt treatment. We estimated that approximately 1 ng of GST fusion proteins could bind to 50 µg of total proteins present in EE. Figure 1 also reveals a higher membrane attachment efficiency of the GSTrab4Q67L mutant compared to that of the GSTrab4S22N mutant. This is possibly the consequence of the interaction of the GSTrab4S22N mutant with cytosolic rabGDI, preventing membrane interactions (27,32). In contrast, GSTrab4CT3, which lacks its prenylation site, was unable to associate with EE. In summary, these results demonstrate that recombinant rabGTPases can be prenylated in vitro, allowing membrane attachment.

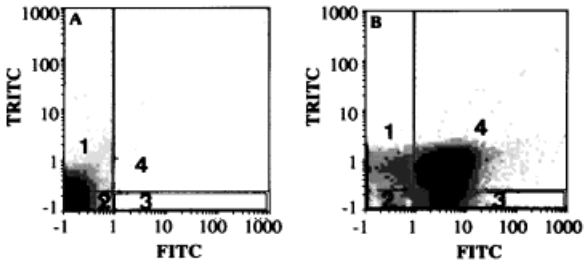

FIG. 2. Distribution of rab4 and rab5 on EE membrane vesicles. EE were incubated with affinity-purified antirab4 or murine monoclonal anti-rab5 antibodies and counterstained with Fab'_2 goat anti–rabbit IgG fluorescein-labeled and Fab'_2 goat anti–mouse IgG rhodamine-labeled antibodies (**B**). In control samples (**A**), rabbit polyclonal anti-human CD26 and mouse monoclonal anti-lysozyme antibodies were used instead of rabbit anti-rab4 and mouse antirab5 antibodies, respectively. At the end of reactions, samples were analyzed with an Elite flow cytometer. The laser excitation for fluorescein was 488 nm and 514 nm for rhodamine. FITC, fluorescence channel; TRITC, rhodamine channel; 50,000 EE were analyzed for A and B. Total EE populations were separated in four quadrants. Quadrant 1, TRITC-labeled EE; quadrant 2, double-negative EE; quadrant 3, FITC-labeled EE; quadrant 4, double-positive EE.

Flow Cytometric Assay Allows the Detection of EE Membrane Fusion

We developed a novel in vitro assay monitored by flow cytometry to evaluate quantitatively both the distribution of the rab4 and rab5 small GTPases on EE and their effects on EE membrane dynamics when added exogenously as GSTrab fusion proteins.

Distribution of rab4 and rab5 GTPases on EE. Dual immunofluorescence was performed to determine quantitatively the distribution of rab4 and rab5GTPases on EE. Results presented in Figure 2 show that EE representing 61.6% of the total EE population (Fig. 2B, quadrant 4) express both rab4 and rab5 on their membranes. This demonstrates a partial overlap in the distribution of these early endosomal rab proteins on membrane fractions, corroborating immunolocalization results (6). When FITC-BSA was internalized for 5 min at 37°C, more than 90% of the FITC-BSA-containing elements were positive for both rab4 and rab5, suggesting that, after 5 min of internalization, the fluorescent marker was located mainly in a compartment containing the two GTPases (not shown). We took advantage of these observations to study the effects of recombinant rab4 protein on the formation of triple-labeled organelles using anti-rab5 antibodies. Conversely, we used anti-rab4 antibodies to assay the effects of recombinant rab5 protein on endosome fusion.

Flow cytometric analysis after in vitro assay and FRET measurements. FITC-BSA and TRITC-BSA were internalized for 5 min at 37°C in two separate populations of BHK cells. EE containing FITC-BSA or TRITC-BSA were prepared and incubated together at 37°C in the presence of cytosol and an ATP-regenerating system after a preincubation of 10 min at 4°C. After various periods of time, reactions were stopped. The small GTPases rab4 or rab5 were detected with specific antibodies revealed with a

streptavidin-APC system, which emits fluorescence at a longer wavelength than FITC or TRITC, allowing the simultaneous detection of all three fluorophores. The flow cytometer was calibrated for the best separation of 0.95 μm, 2 μm, and 5 μm fluorescent beads both in the forward angle light scatter and right angle light scatter modes. To control the EE size distributions before and after in vitro assays, samples were analyzed with a fluorescence imaging microscope, ACAS 470 (Meridian Inc., Okemos, MI). The size distribution of EE added initially to the reaction assay was found to be unimodal, ranging from 0.5 to 3 μm average diameter, with a mean value of 1.5 μm (not shown), in agreement with the average size of early endosomes measured by electron microscopy and obtained after subcellular fractionation (11,13,14). After 15 min at 37°C, some 3–7 μm EE were observed (not shown). Based on the size differences controlled by fluorescence imaging (not shown), gates were set up to discriminate EE subpopulations ranging between 1 and 7 μm (total EE population), between 1 and 3 μm (1–3 μm EE) and between 3 and 7 μm (3–7 μm EE).

We first determined the kinetics of appearance of triple-labeled EE (FITC-BSA, TRITC-BSA, and APC-stained anti-rab5 or anti-rab4). After a 10 min preincubation at 4°C, a small number of triple-labeled EE were detected (Fig. 3A, 0 min). In contrast, when the temperature was raised to 37°C, the number of detected triple-labeled EE increased and reached a plateau from 15 min onwards (Fig. 3A), demonstrating that the formation of triple-labeled EE is temperature dependent.

Because flow cytometric measurements could not discriminate between fusion or aggregation of EE, we used FRET measurements to discriminate between aggregation or fusion, leading to intermixing of membranes and content. We evaluated the energy transfer efficiency for each EE, from which a frequency distribution for the population was generated. In samples incubated for 10 min at 4°C, no FRET was observed (Fig. 4A), suggesting that the structures observed at 4°C very likely corresponded to aggregates rather than fused endosomes. After 15 min at 37°C, a large increase in FRET efficiency to 11.4 was seen (Fig. 4B), indicating a close proximity of the two fluorophores generated after membrane fusion. After 60 min at 37°C, a FRET efficiency very similar to that observed after 15 min was observed (data not shown). In these experiments, donor/acceptor molar ratio was determined as described in Materials and Methods. The donor/acceptor molar ratio used for Figure 4 was equal to 1. FRET experiments clearly demonstrate that membrane fusion occurred during in vitro assays at 37°C and not aggregation.

Figure 3A also shows that the fusion activity monitored by our flow cytometry assay was strongly increased by rab5, as has been described for the case in vitro and in vivo

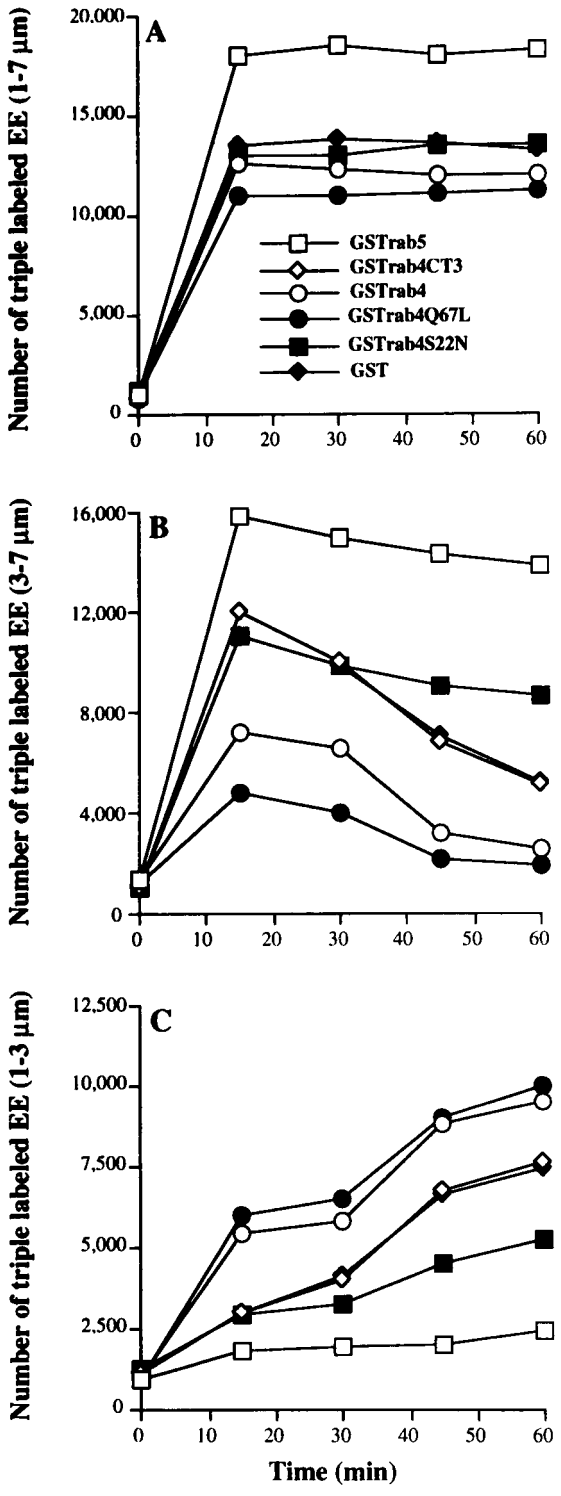

FIG. 3. Quantitation of the effects of rab4 and 5 on the two classes of EE subpopulations. In vitro assays were carried out for 10 min at 4°C (0 min) prior to 15, 30, 45, and 60 min incubations at 37°C in the presence of an ATP-regenerating system and 8 μM geranylgeranyl-pyrophosphate, supplemented with 1.5 μg of GST, GSTrab5, GSTrab4, GSTrab4CT3, GSTrab4S22N, or GSTrab4Q67L. From each sample, we analyzed 33,000 elements. Statistical analyses of the number of EE positive for rab4 or rab5 and containing both FITC- and TRITC-BSA were performed with the PRISM software of the Elite flow cytometer (see Materials and Methods). For **A**, the total EE population ranging between 1 and 7 μm was analyzed. In contrast, a gate was chosen in the light scattered modes (FALS and 90LS) to select the 3–7 μm EE (**B**) or the 1–3 μm EE (**C**). One point represents the average value of nine different experiments.

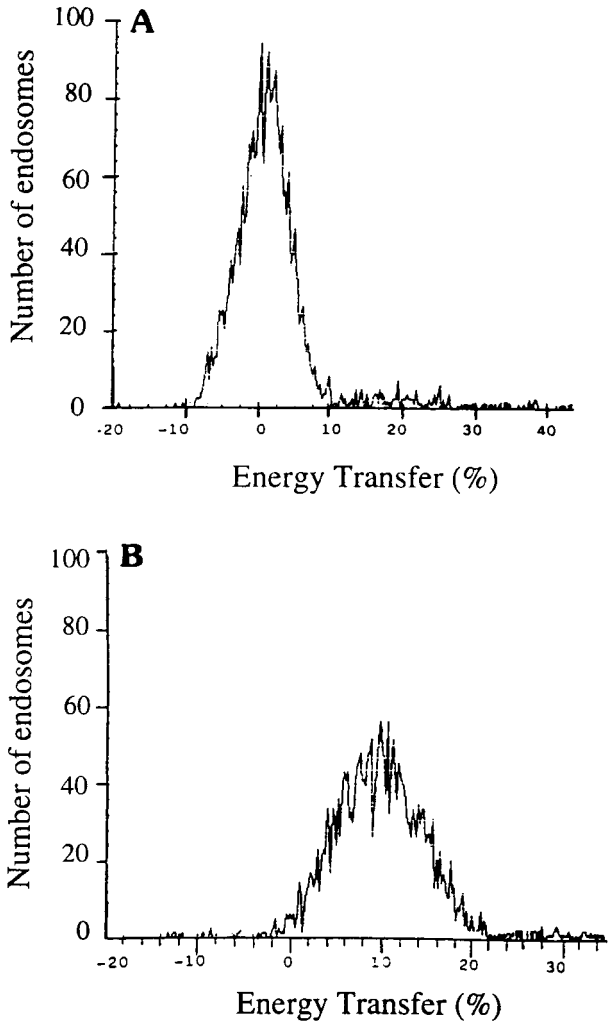

FIG. 4. FRET analyses on fused EE. EE containing FITC-BSA or TRITC-BSA were complemented with cytosol, an ATP-regenerating system, and 8 μM geranylgeranyl-pyrophosphate and incubated for 10 min at 4°C or 15 min at 37°C. **A:** Frequency distribution of energy transfer efficiency between FITC-BSA and TRITC-BSA in EE after 10 min at 4°C (mean 0.2%). No significant transfer was observed at 4°C. **B:** Frequency distribution of energy transfer efficiency between FITC-BSA and TRITC-BSA in EE after 15 min at 37°C (mean 11.4%) showing a significant energy transfer. Approximately 5,000 EE were analyzed per distribution. FITC to TRITC ratio was 1 in both cases.

(3,11). In contrast, GSTrab4 and GSTrab4CT3 did not have any effect (Fig. 3A). Only a slight inhibition was observed when assays were carried out in the presence of the GSTrab4Q67L mutant.

These results show that rab4 exerts no significant effects on the kinetics and extent of early endosome fusion, suggesting that this small GTPase is not an essential protein for early endosome fusion in vitro.

rab4 Controls the Appearance of Small Fused EE

The flow cytometric assay was used next to look at the effects of the GSTrab fusion proteins on the 1–3 and 3–7 μm EE subpopulations defined above. Quantifications for both 3–7 and 1–3 μm EE are given in Figure 3B,C, respectively. In all conditions, after 10 min at 4°C, a small number of triple-labeled EE, which never exceeded 1,000 elements, was detected (Fig. 3B,C). In control experiments carried out in the presence of *E. coli*-produced GST moiety alone (GST), the number of 3–7 μm EE significantly increased before 15 min of incubation at 37°C (Fig. 3B) but declined between 15 and 60 min at 37°C, paralleling the appearance of the small 1–3 μm EE (Fig. 3C). As expected, the formation of large 3–7 μm EE was stimulated by recombinant rab5, and most of the EE persisted as 3–7 μm structures (Fig. 3B), whereas the formation of 1–3 μm EE was minimal (Fig. 3C). This demonstrates that rab5 locked EE in a 3–7 μm fused state, as has been reported in vivo (3). In contrast, GSTrab4Q67L with a low rate of GTP hydrolysis, produced a twofold decrease in the number of triple-labeled 3–7 μm EE (Fig. 3B) compared to control. A similar albeit less pronounced effect was observed in the presence of wild-type GSTrab4. Interestingly, the decrease in the number of large EE was concomitant with the increase of small EE (Fig. 3B,C), suggesting a precursor-product relationship between 3–7 μm EE and 1–3 μm EE.

In addition, and even though it did not have any effect on the formation of 3–7 μm EE (Fig. 3B), the rab4S22N mutant partially prevented the formation of the 1–3 μm EE (Fig. 3C). GSTrab4CT3 had no effect (Fig. 3B,C). Altogether, these results indicate that rab4 has no effect on EE fusion but rapidly promotes the generation of 1–3 μm triple-labeled EE, very likely from the 3–7 μm EE subpopulation.

Rab4 Induces the Fission of Isolated Large Triple-Labeled EE

To confirm this hypothesis, large EE fusion intermediates were preformed with a 15 min incubation at 37°C, isolated by fluorescence-activated cell sorting, and then reincubated with cytosol and rab4 mutants. Large EE were selected for having a 3–7 μm size (Fig. 5A) and containing the two fluorescent markers (FITC- and TRITC-BSA; Fig. 5B). For quantitative analyses, we selected an initial population of double-labeled large EE representing 4.8% of the total membrane population that did not contain any single labeled structures (Fig. 5Ea). During sorting, large EE were directly collected in cold cytosol, and double-labeled large EE were checked by flow cytometry for both size (Fig. 5C) and fluorescence (Fig. 5D). They represented 46.3% of the total sorted population, corresponding to a tenfold enrichment (Fig 5Eb). Under these conditions, the integrity of the membranes was conserved, allowing a subsequent incubation of the sorted large EE for 10 min at 37°C in the absence (Fig. 5Ec) or the presence (Fig. 5Ed) of 1.5 μg GSTrab4Q67L or 1.5 μg of GSTrab4S22N (Fig. 5Ee). These experiments document that the rab4Q67L mutant induces a rapid fission of the large EE (Fig. 5Ed) concomitant with the appearance of small triple-labeled EE (not shown), confirming that the large EE are the primary target of rab4 in the assay.

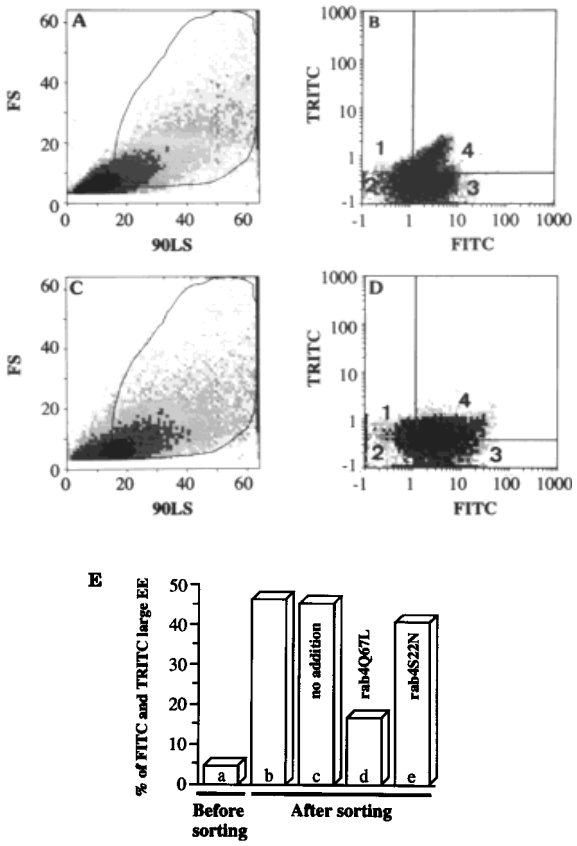

FIG. 5. Effect of rab4 on isolated large EE. EE containing FITC-BSA or TRITC-BSA were obtained as described in Materials and Methods. In vitro assays were initiated by a 10 min incubation at 4°C followed by 15 min at 37°C. Then, samples were chilled to 4°C and sorting conditions were set up. Large EE were selected by gating on both their 3–7 μm size in the light scatter modes (**A**) and the presence of FITC-BSA and TRITC-BSA contents (**B**). Isolated large EE were collected in cold cytosol and immediately checked for their sorting efficiency in both their size (**C**) and fluorescence emissions (**D**). Quantitations are given in **E** before (Ea) and after (Eb) sorting. Isolated EE were then reincubated for 10 min at 37°C in the absence (Ec) or in the presence of 1.5 μg GSTrab4Q67L (Ed) or GSTrab4S22N (Ee). Results are expressed as the percentage of double-labeled (FITC and TRITC) 3–7 μm EE over the total membrane population; 50,000 EE were analyzed in each cytogram. Quadrant 1, TRITC-labeled EE; quadrant 2, double-negative EE; quadrant 3, FITC-labeled EE; quadrant 4, double-positive EE.

DISCUSSION

In this paper, we describe a three-color flow cytometric assay that was developed to monitor early endosomal membrane dynamics in vitro. This method allowed us to detect simultaneously the presence of two internalized fluid-phase endocytic tracers and the early endosomal marker proteins rab4 or rab5 (4,33). We show here that early endosome membrane dynamics can be dissected in vitro into discrete fusion and fission steps controlled by the rab4 and rab5 GTPases.

Previous studies showed that rab5 controls the internalization of solutes and ligands from the plasma membrane into early endosomes and the homotypic fusion between individual early endosome elements (3,11). The role of rab5 in homotypic early endosome fusion has been documented in biochemical assays (11) and was confirmed by electron microscopic observations showing that overexpression of wild-type rab5 in BHK cells leads to the specific increase in the size of early endosomes (3). This phenotype was enhanced upon overexpression of the GTPase-deficient mutant rab5Q79L (28). Expression of this mutant protein in BHK cells generated early endocytic structures that were even larger than those observed upon wild-type rab5 overexpression, suggesting that hydrolysis of rab5-bound GTP is required after membrane fusion to inactivate the protein.

We first ascertained that the recombinant GSTrab proteins possessing a carboxyterminal prenylation site could attach to endosomal membranes. Indeed, GSTrab4Q67L, GSTrab4S22N, and GSTrab5wt were found to associate with early endosomes under the conditions of the in vitro assay. In contrast, GST used as a control or GSTrabCT3 could not bind to EE and had no effect on EE membrane fusion and fission mechanisms, corroborating several data showing that membrane attachment is a prerequisite for rab protein function in intracellular membrane transport (3,11,22,28). When recombinant rab5 was added to the assay, most of the early endosome structures were blocked at the ''intermediate'' stage of large endosomes (Fig. 3). In contrast, in control incubations lacking exogenous rab5, the large (3–7 μm) endosome population quickly disappeared, to give rise to a small (1–3 μm) early endosomal subpopulation containing the two separately internalized fluorescent markers (FITC-BSA and TRITC-BSA), indicating that the small endosomes were subsequently generated from the population of 3–7 μm fused endosomes by a membrane fission process. Strikingly, rab4 stimulated the formation of small triple-labeled EE from the 3–7 μm isolated large fusion intermediates, a process that was enhanced by the GTP hydrolysis mutant rab4Q67L (Fig. 5).

The picture that emerged from our in vitro assay suggests that the individual elements of the early endosomal system communicate through fusion and fission events. The fission process can be interpreted either as a homotypic event or as a budding process, generating vesicles destined to be targeted to other organelles within the cell. At least two models can be proposed to explain our results. In the first mechanism, fusion and fission are viewed as homotypic events in which individual early endosomal elements containing both rab5 and rab4 fuse with each other to generate larger endosomal structures. This step is controlled by rab5. Upon hydrolysis of associated GTP, the fusion machinery may be activated and rab5 with bound GDP is released in the cytosol (28). Subsequently, fission may take place, stimulated by rab4 with bound GTP, leading to the regeneration of small endosomal structures. The consequence of this sequential fusion-fission process is a mixing of both membrane and contents of the individual endosomal elements. When the rab5Q79L or rab4Q67L mutants with reduced GTPase activity are introduced into this system, they may shift the early endosome membrane equilibrium towards the large fused endosomal structures or to the small endosomal

structures with mixed content and membrane, respectively.

However, this model does not take into account the fact that 25% of early endosomes contain rab4 only, indicating that rab4 is present at least on two endosomal subdomains. Therefore, a second mechanism can be hypothesized. In this model, the hydrolysis of rab5-associated GTP first controls homotypic fusion of early endosomes. Then, from the fused EE step, at least two possibilities emerge. One implies that the hydrolysis of rab4-associated GTP is required for a direct budding of the rab4-positive recycling compartment from fused EE, postulating that a rab protein might be involved in a budding event as rab1b for vesicle formation between ER and Golgi and intra-Golgi transport (21). Another hypothesis would be that, after generation of fused EE, small vesicles, not detectable with our analysis system, would be generated and able to fuse with the rab4-positive recycling compartment. The budding of these vesicles might be controlled by GTPases other than rabs. For instance, one candidate is Arf6; that GTPase was shown to be involved in the transferrin recycling pathway (7,20). rab4 would then control the fusion of these small vesicle intermediates with the recycling compartment.

ACKNOWLEDGMENTS

The authors thank members of our laboratories for thoughtful discussions. Koert Burger is especially thanked for careful reading of the manuscript and Nicole Brun-Roubereau for initiating flow cytometry experiments on endosomes. P.v.d.S. is an investigator of the Netherlands Academy of Arts and Sciences.

LITERATURE CITED

1. Aniento F, Emans N, Griffiths G, Gruenberg J: Cytoplasmic dynein-dependent vesicular transport from early to late endosomes. J Cell Biol 123:1373–1388, 1993.
2. Bradford MM: A rapid and sensitive method for the quantitation of microgram quantities of protein utilizing the principle of protein-dye binding. Anal Biochem 72:248–254, 1976.
3. Bucci C, Parton R, Mather I, Stunnenberg H, Simons K, Zerial M: The small GTPase rab5 functions as a regulatory factor in the endocytic pathway. Cell 70:715–728, 1992.
4. Chavrier P, Parton RG, Hauri HP, Simons K, Zerial M: Localization of low molecular weight GTP binding proteins to exocytic and endocytic compartments. Cell 62:317–329, 1990.
5. Chavrier P, Vingron M, Sander C, Simons K, Zerial M: Molecular cloning of YPT1/SEC4-related cDNAs from an epithelial cell line. Mol Cell Biol 10:6578–6585, 1990.
6. Daro E, van der Sluijs P, Galli T, Mellman I: rab4 and cellubrevin define different early endosome populations on the pathway of transferrin receptor recycling. Proc Natl Acad Sci USA 93:9556–9564, 1996.
7. D'Souza-Schorey C, Li G, Colombo MI, Stahl PD: A regulatory role for ARF6 in receptor-mediated endocytosis. Science 267:1175–1178, 1995.
8. Gennis LS, Gennis RB, Cantor CR: Singlet energy-transfer studies on associating protein systems: Distance measurements on trypsin, α-chymotrypsin and their protein inhibitors. Biochemistry 11:2509–2516, 1972.
9. Goda Y, Pfeffer SR: Cell-free systems to study vesicular transport along the secretory and endocytic pathways. FASEB J 3:2488–2495, 1989.
10. Gorvel JP, Mishal Z, Liegey F, Rigal A, Maroux S: Conformational change of rabbit aminopeptidase N into enterocyte plasma membrane domains analyzed by flow cytometry fluorescence energy transfer. J Cell Biol 108:2193–2200, 1989.
11. Gorvel JP, Chavrier P, Zerial M, Gruenberg J: Rab5 controls early endosomes fusion in vitro. Cell 64:915–925, 1991.
12. Gruenberg J, Howell KE: Membrane traffic in endocytosis: insights from cell-free assays. Annu Rev Cell Biol 5:453–481, 1989.
13. Gruenberg J, Griffiths G, Howell K: Characterization of the early endosome and putative endocytic carrier vesicles in vivo and with an assay of vesicle fusion in vitro. J Cell Biol 108:1301–1316, 1989.
14. Griffiths G, Back R, Marsh M: A quantitative analysis of the endocytic pathway in baby hamster kidney cells. J Cell Biol 109:2703–2720, 1989.
15. Haaijman JJ, Van Dalen JPR: Quantification in immunofluorescence microscopy. A new standard for fluorescein and rhodamine emission measurements. J Immunol Methods 5:359–374, 1974.
16. Hopkins CR, Gibson A, Shipman M, Miller K: Movement of internalized ligand-receptor complexes along a continuous endosomal reticulum. Nature 346:335–339, 1990.
17. Lenhard JM, Kahn RA, Stahl PD: Evidence for ADP-ribosylation (ARF) as a regulator of in vitro endosome-endosome fusion. J Biol Chem 267:13047–13052, 1992.
18. Lombardi D, Soldati T, Riederer M, Zerial M, Pfeffer S: Rab9 functions in transport between late endosomes and the trans Golgi network. EMBO J 12:677–682, 1993.
19. Olkkonen VM, Dupree P, Killisch I, Lütcke A, Zerial M, Simons K: Molecular cloning and subcellular localization of three GTP-binding proteins of the rab subfamily. J Cell Sci 106:1249–1261, 1993.
20. Peters PJ, Hsu VW, Ooi CE, Finazzi D, Teal SB, Oorshot V, Donaldson JG, Klausner RD: Overexpression of wild-type and mutant ARF1 and ARF6: Distinct perturbations of nonoverlapping membrane compartments. J Cell Biol 128:1003–1017, 1995.
21. Plutner H, Cox AD, Pind S, Far RK, Bourne JR, Schwaninger R, Der CJ, Balch WE: rab1b regulates vesicular transport between the endoplasmic reticulum and successive golgi compartments. J Cell Biol 115:31–43, 1991.
22. Robinson MS, Watts C, Zerial M: Membrane dynamics in endocytosis. Cell 84:13–21, 1996.
23. Rodriguez L, Stirling CJ, Woodman PG: Multiple N-ethylmaleimide-sensitive components are required for endosomal vesicle fusion. Mol Biol Cell 5:773–783, 1994.
24. Rothman JE: Mechanism of intracellular transport. Nature 372:55–62, 1994.
25. Rothman JE, Warren G: Implication of the SNARE hypothesis for intracellular membrane topology and dynamics. Curr Biol 4:220–233, 1994.
26. Sanger F, Niklen S, Coulson AR: DNA sequencing with chain-terminating inhibitors. Proc Natl Acad Sci USA 74:5463–5467, 1977.
27. Soldati T, Shapiro AD, Dirac Svejstrup AB, Pfeffer SR: Membrane targeting of the small GTPase rab9 is accompanied by nucleotide exchange. Nature 369:76–78, 1994.
28. Stenmark H, Parton R, Steele-Mortimer O, Lütke A, Gruenberg J, Zerial M: Inhibition of rab5 GTPase activity stimulates membrane fusion and endocytosis. EMBO J 13:1287–1296, 1994.
29. Szöllosi J, Matyus L, Tron L, Balazs M, Ember I, Fulwyler MJ, Damjanovich S: Flow cytometric measurements of fluorescence energy transfer using single laser excitation. Cytometry 5:210–216, 1987.
30. Tooze J, Hollinshead M: Tubular early endosomal networks in AtT20 and other cells. J Cell Biol 115:635–653, 1991.
31. Tron L, Szöllosi J, Damjanovich S, Helliwell SH, Arndt-Jovin DH, Jovin TM: Flow cytometry measurements of fluorescence resonance energy transfer on cell surface: Quantitative evaluation of the transfer efficiency on a cell-by-cell basis. Biophys J 45:939–946, 1984.
32. Ullrich O, Horiuchi H, Bucci C, Zerial M: Membrane association of rab5 mediated by GDP-dissociation inhibitor and accompanied by GDP/GTP exchange. Nature 368:157–160, 1994.
33. van der Sluijs P, Hull M, Zahraoui A, Tavitian A, Goud B, Mellman I: The small GTP-binding protein rab4 is associated with early endosomes. Proc Natl Acad Sci USA 88:6313–6317, 1991.
34. van der Sluijs P, Hull M, Huber L, Male P, Goud B, Mellman I: EMBO J 11:4379–4389, 1992.
35. van der Sluijs P, Hull M, Webster P, Goud B, Mellman I: The small GTP-binding protein rab4 controls early sorting event on the endocytic pathway. Cell 70:729–740, 1992.